

A 4-DOF Robot for Positioning Ultrasound Imaging Catheters

Paul M. Loschak *

Student Member of ASME
Graduate Research Assistant
Harvard Biorobotics Laboratory
Paulson School of Eng. and App. Sci.
Harvard University
Cambridge, Massachusetts 02138
Email: loschak@seas.harvard.edu

Alperen Degirmenci

Student Member of ASME
Graduate Research Assistant
Harvard Biorobotics Laboratory
Paulson School of Eng. and App. Sci.
Harvard University
Cambridge, Massachusetts 02138
Email: adegirmenci@seas.harvard.edu

Yaroslav Tenzer

Affiliate
Harvard Biorobotics Laboratory
Paulson School of Eng. and App. Sci.
Harvard University
Cambridge, Massachusetts 02138
Email: ytenzer@seas.harvard.edu

Cory M. Tschabrunn

Technical Director
Experimental Electrophysiology
Division of Cardiovascular Medicine
Beth Israel Deaconess Medical Center
Boston, Massachusetts 02215
Email: cory.tschabrunn@bidmc.harvard.edu

Elad Anter

Director
Experimental Electrophysiology
Division of Cardiovascular Medicine
Beth Israel Deaconess Medical Center
Boston, Massachusetts 02215
Email: eanter@bidmc.harvard.edu

Robert D. Howe

Professor
Harvard Biorobotics Laboratory
Paulson School of Eng. and App. Sci.
Harvard University
Cambridge, Massachusetts 02138
Email: howe@seas.harvard.edu

In this paper we present the design, fabrication, and testing of a robot for automatically positioning ultrasound imaging catheters. Our system will point ultrasound (US) catheters to provide real-time imaging of anatomical structures and working instruments during minimally invasive procedures. Manually navigating US catheters is difficult and requires extensive training in order to aim the US imager at desired targets. Therefore, a four DOF robotic system was developed to automatically navigate US imaging catheters for enhanced imaging. A rotational transmission enables three DOF for pitch, yaw, and roll of the imager. This transmission is translated by the fourth DOF. An accuracy analysis calculated the maximum allowable joint motion error. Rotational joints must be accurate to within 1.5° and the translational joint must be accurate within 1.4 mm. Motion tests then validated the accuracy of the robot. The average resulting errors in positioning of the rotational joints were $0.04^\circ - 0.22^\circ$. The average measured backlash was $0.18^\circ - 0.86^\circ$. Measurements of average translational positioning and backlash er-

rors were negligible. The resulting joint motion errors were well within the required specifications for accurate robot motion. The output of the catheter was then tested to verify the effectiveness of the handle motions to transmit torques and translations to the catheter tip. The catheter tip was navigated to desired target poses with average error 1.3 mm and 0.71° . Such effective manipulation of US imaging catheters will enable better visualization in various procedures ranging from cardiac arrhythmia treatment to tumor removal in urological cases.

1 Introduction

Long, thin flexible instruments such as catheters are used to perform an ever-increasing range of minimally invasive procedures. Catheters are advantageous because it is possible to gain surgical access to difficult-to-reach anatomical regions with significantly less trauma to the patient when compared with conventional surgical techniques. However, catheters are difficult to manipulate precisely, and naviga-

*Address all correspondence to this author.

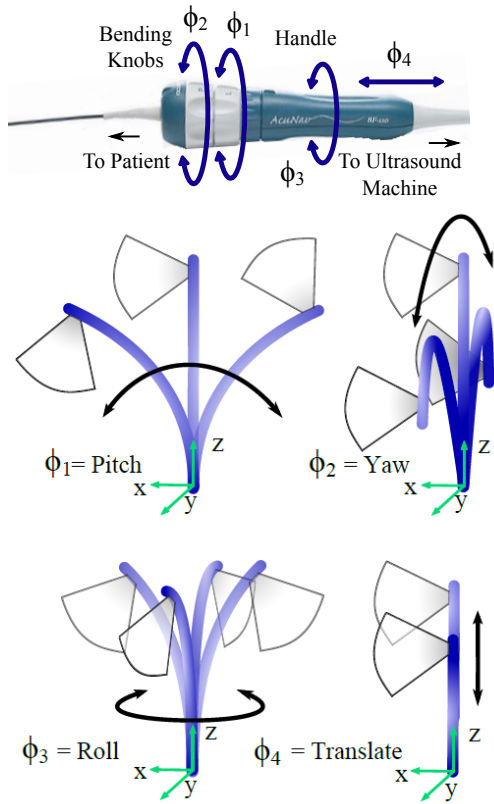


Fig. 1. Catheter handle degrees of freedom and resulting catheter tip motions

tional imaging options are limited by expense and clinical feasibility. Therefore, these instruments are limited in functionality to performing mostly simple tasks that do not require high positioning accuracy. For example, stent placement and balloon angioplasty [1] are tasks which require careful placement in 1D, but do not involve accurate 3D navigation or dexterous manipulation of tissue.

Ultrasound (US) imaging catheters, which contain an US transducer at the distal tip of the catheter, are useful for acquiring images from within the patient and assisting in navigation. They can provide high-resolution views of anatomical structures and working instruments. Used routinely for over a decade in clinical practice [2], US catheters are advantageous in comparison with external probes because targets can be visualized with higher acoustic frequencies in the near-field. Signals from external probes provide lower quality imaging due to attenuation by intervening layers of muscle, fat, and other tissue. However, the difficulty in manually controlling these US catheters is a disadvantage compared to external probes. Clinicians maneuver US catheters by adjusting control knobs (connected to the catheter tip by pull wires) and advancing/rotating the catheter handle (Fig. 1). Steering the US imager and aligning the plane with a target to obtain adequate views is a challenging and time-consuming process. Therefore, many clinicians prefer to only use US catheters while performing critical tasks. An example of a critical task is septal puncture [1], in which the risk of atrial perforation and subsequent morbidity is high.

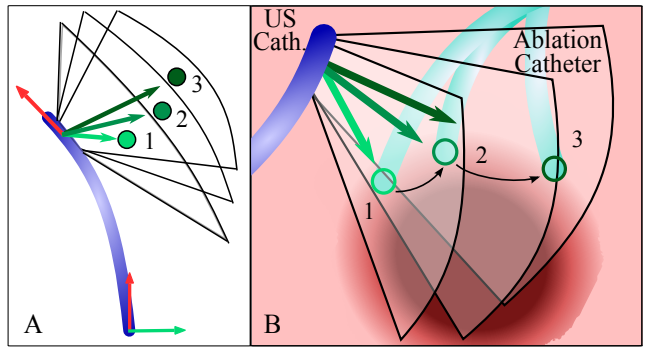


Fig. 2. (A) Catheter motion during panorama image collection. (B) Instrument tracking: adjustment of imaging plane to visualize ablation catheter tip.

To increase the utility of these high-quality imaging devices, we developed a robotic system for automatically guiding US imaging catheters within the heart. The system was used to demonstrate millimeter-level positioning accuracy and sub-degree-level angular steering accuracy in bench-top experiments. These techniques enabled complex control of the US catheter to be performed with simple commands. For example, the system was used to rotate the US imager about its own axis without displacing the catheter (Fig. 2 (left)). This is useful for collecting a series of 2D images and reconstructing high-quality 3D and 4D volumes (3D + time) for procedure guidance or diagnosis while keeping the US catheter fixed in a safe location. The system is also able to align the US plane with working instruments inside the heart. As instruments are navigated throughout the workspace, the system maintains imager alignment, enabling constant visualization of instrument-tissue interactions (Fig. 2 (right)).

The details of the control and navigation of the system, as well as bench top validation data, are presented in our previous work [3–5]. The work presented in this paper focuses primarily on the physical implementation of the robotic system, which manipulates the catheter handle for accurate navigation. In our previous work, the physical implementation of the system was designed for initial prototyping of the robotic system and demonstrating the imager-steering functionality [3,6]. As the US catheter steering system was made ready for testing in animal models it was necessary to design, fabricate, and test a new method for mating actuators to the catheter handle. The updated robot design is smaller, lighter, more portable, and more robust. US catheters can be inserted, clamped into the robot, and removed within 10 seconds. Features mating to the catheter shaft assist in guiding motion to improve efficiency and prevent catheter buckling. The following sections of this paper begin with an overview of the robotic system. The transmission of the catheter steering robot is presented and the motion of each joint is characterized to verify positioning accuracy. The new four degree of freedom (4-DOF) robot for positioning US imaging catheters is robust, easily integrates with existing clinical practices, and will enable safe US imaging in a range of surgical procedures.

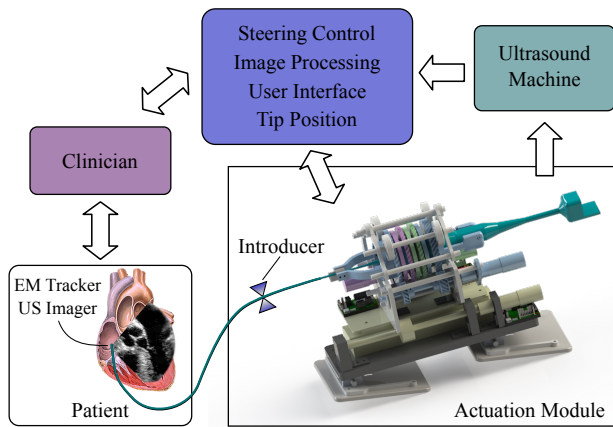


Fig. 3. US catheter robotic system

2 Background

This paper focuses on the design, fabrication, and testing of the actuation module which manipulates the catheter. However, the actuation module is one component of a larger robotic system (Fig. 3) for steering US catheters to provide enhanced US imaging for clinicians. The system consists of the following parts:

1. Actuation module (“robot”)
2. Steering control
3. Image processing
4. User interface
5. Catheter tip position sensing
6. Ultrasound machine

The position and orientation of the catheter tip are controlled by sensing the catheter pose and adjusting the actuator commands in an iterative loop until the desired pose is reached. The pose is sensed by electromagnetic (EM) trackers attached to the tip of the catheter. The steering control module (described in previous work [3, 4]) directs the motion of the US catheter tip. EM sensor values and inverse kinematics-based calculations are used to determine actuator commands. The kinematic model describes the relationships between the imaging plane orientation, tip location, and catheter controls. A data acquisition card is used to record the ECG signal. The US machine, which displays US images to the clinician, is also connected to the computer through a frame grabber. The computer contains an image processing module for recording 2D images and reconstructing useful panoramas of anatomical regions. User control of the robot is done via a graphical user interface (GUI) on a computer terminal, through which the user can enter commands to move the robot in joint space, tip space, or begin automated tasks, such as instrument tracking. Additional automated tasks include imaging designated regions of anatomy and collecting views of target structures from multiple angles. If desired, the user can simply and quickly detach the catheter from the robot to manually navigate the catheter.

The system presented in this paper provides functionality that is different from commercially available catheter robots. Existing systems such as the Amigo (Catheter Robotics, USA) and CorPath (Corindus, USA) simply repli-

cate manual joint space control knobs and allow clinicians to remotely teleoperate the catheter from a shielded room [7, 8]. This improves comfort and reduces radiation exposure to the operator from fluoroscopic imaging, but does not reduce the difficulty in understanding the necessary knob adjustments needed to navigate catheters. The Artisan (Hansen Medical, USA), EPOCH/V-Drive (Stereotaxis, USA), and several research-level prototypes of flexible manipulator systems feature Cartesian control, but they do not control the orientation of the catheter, which is necessary for aiming the US imager [9–16]. By fully articulating the four DOFs of US catheters, our system is able to control the position of the catheter and one DOF of its orientation.

3 Design Requirements

The robot must be designed to position 4-DOF US imaging catheters in an operating room setting. The actuators must mate with the handle of any intracardiac echocardiography (ICE) catheter (Biosense Webster, USA), and the mating profile should be easily adjusted to fit other types of catheter handles. The roll axis must allow for continuous rotation. Plastic drapes for use in the clinic must not interfere with handle actuation.

The robot must be clinician-friendly for the insertion and removal of catheters. In a typical procedure the clinician connects the US catheter to the US machine, manually introduces the US catheter to the vasculature, and then manually navigates the tip of the catheter to the general region of interest. In the robotic procedure the clinician must be able to then disconnect the US machine cable, insert the catheter handle into the robot, secure the catheter in place, and reattach the US machine cable. A clinician with minimal experience in robotics should be able to connect the catheter to the robot (or remove the catheter from the robot) within 10 seconds.

Catheters are guided into the vasculature through an introducer, which is a plastic tube containing a rubber seal that prevents blood leakage. The introducer hinders rotational and translational movements of the catheter shaft due to friction against the seal. Clinicians compensate for this by us-

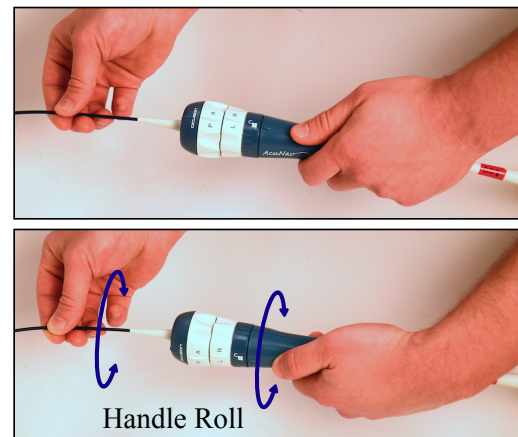


Fig. 4. Manual manipulation of handle roll requires coordinated two-handed movements

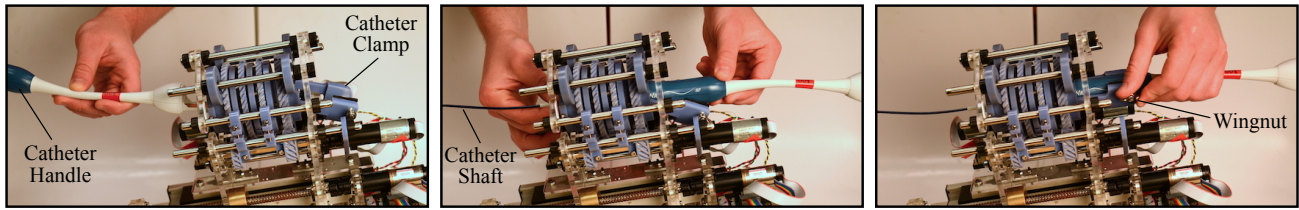


Fig. 5. A demonstration of catheter attachment to the robotic system. Attachment and detachment takes less than 10 seconds.

ing one hand to manipulate the catheter handle and another hand to grasp the catheter shaft (Fig. 4). The two-handed technique increases the amount of torque transmitted to the catheter tip during rotation. It also prevents the catheter from buckling outside the patient during insertion. The robot must be designed with features to assist in catheter shaft rotation and to prevent shaft buckling.

The accuracy requirements of the robot are determined by the sensors used for steering the catheter tip. Measurements from the electromagnetic (EM) tracker at the tip of the catheter enable the controller to know the full pose of the US imager. The accuracy of the US imager pose is limited by the accuracy of the EM tracking system (trakSTAR, Northern Digital Inc., Canada; 1.4 mm position and 0.5° orientation accuracy). The relationship between the joint inputs and the catheter tip bending output is sensitive such that a 1.5° change in the pitch or yaw joints produces an average 1.4 mm motion accuracy at the tip. Therefore, it is important that the robot is able to adjust the rotational joint inputs to the desired angle within 1.5° and to adjust the translational joint within 1.4 mm. This level of accuracy is sufficient for navigating the US imager to the desired location and pointing in the desired direction.

4 Robot Design

The robot was designed to manipulate the 4 DOFs of the catheter handle (Fig. 1). The translational DOF (ϕ_4) translates the catheter along its axial direction. This motion is necessary for advancing or retracting the catheter further into or out of the patient. A bending DOF twists the “L/R” (pitch, ϕ_1) knob to create a catheter bending motion and pitch the US imager. The other bending DOF twists the “P/A” (yaw, ϕ_2) knob to create a catheter bending motion which causes

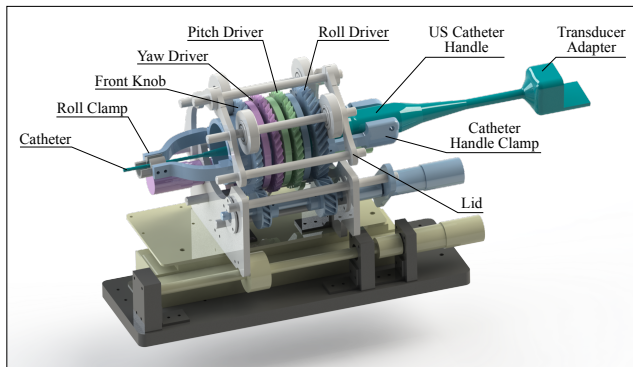


Fig. 6. CAD model of the complete robotic system

the imager to yaw. The last DOF (roll, ϕ_3) rotates the handle of the catheter to produce a roll motion about the long axis of the catheter handle. Hard stops inside the catheter handle limit pitch and yaw axis rotations to $\pm 90^\circ$ relative to the catheter handle. The translation stage was designed to allow 15 cm of travel. These limits are enforced in software with a safety factor to prevent collisions with hard stops. The robot is mounted on two scissor lifts to allow the inclination of the robot to be adjusted for better alignment with the introducer, which helps reduce buckling.

4.1 Catheter Insertion

The catheter is inserted by sliding the proximal end of the handle through the central bore of the transmission (Fig. 5). The catheter handle clamp is rotated downwards on its hinge to avoid obstructing the path of the large transducer adapter. The transmission knobs were designed with inner diameters large enough to allow the transducer adapter to pass through, but small enough to cause a light press fit between the transmission drivers and the catheter knobs. Protrusions on the inside of the transmission drivers mate with matching depressions on the catheter knob (intended for finger pads during manual use). Once the catheter has been fully inserted, the catheter handle clamp is rotated up to mate with the catheter handle (Fig. 6). The clamp is squeezed into place with a light press fit and the connection is tightened by

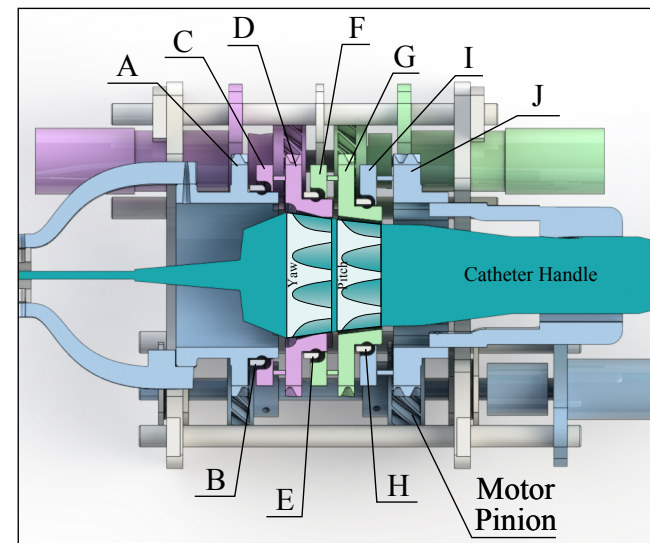


Fig. 7. Cross-sectional view showing knob interactions with the catheter. Parts B, E, H are bearings. Parts B, C, D, E enable yaw; parts E, F, G, H enable pitch; and parts A, B, H, I, J enable roll.

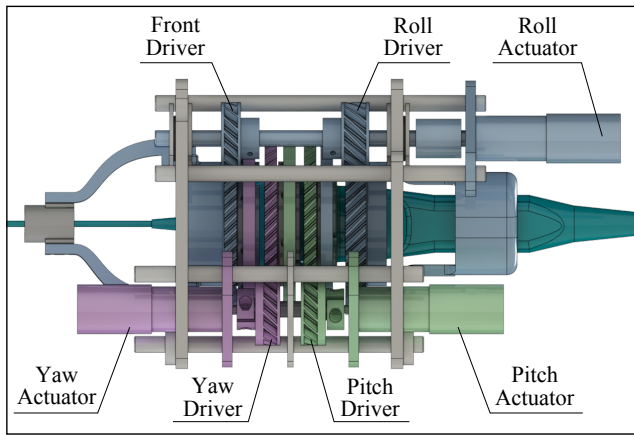


Fig. 8. CAD model showing a detailed bottom view of the rotational transmission

a wingnut.

4.2 Rotational Transmission

The complete robot is shown in Fig. 6. The rotational transmission grasps the catheter handle and manipulates the roll, pitch, and yaw DOFs of the catheter. The transmission consists of four helical gears that are mated coaxially and constrained by ball bearings. The transmission for the pitch and yaw DOFs consists of multiple components (Fig. 7). Components related to yaw motion are colored purple, components related to pitch motion are colored green, and components related to roll motion are colored blue.

Part (D) is a helical gear that is fitted to the P/A knob. Part (E) is a bearing ring which positions eight ball bearings equidistantly around the grooved circumference of the gear (D). Part (F) is a cover to constrain the ball bearings in the axial direction. Each of these three parts can rotate independently of each other. Part (G) of the pitch DOF is another helical gear that is fitted to the L/R knob, and it is fully coupled to Part (F) of the pitch DOF via screws and press-fit pins. Part (H) is a second bearing ring which positions eight balls in place. Part (I) is a second cover which constrains the ball bearings on the pitch driver (G). The roll DOF consists of Part (J), a helical gear mated directly to the catheter handle by a set screw clamp, and is fully coupled to Part (I). Part (A) is the front knob, which mates to the roll clamp to transmit roll torques to the catheter shaft. Part (B) is a third bearing ring, which couples Parts (A) and (C). Part (C) is fully coupled to Part (D). The accuracy of the 3D printed bearing races is examined in the experiments section.

4.3 Actuator Layout

The transmission for the three rotational DOFs was designed such that pitch, yaw, and roll actuators are mechanically attached to the translation stage. This results in a smaller footprint, which is advantageous in the clinical setting. This arrangement also enables an easy method for attaching the catheter to the robot. The coaxial rings create a central bore through which the catheter handle is inserted. The inner diameter of the smallest ring is larger than the

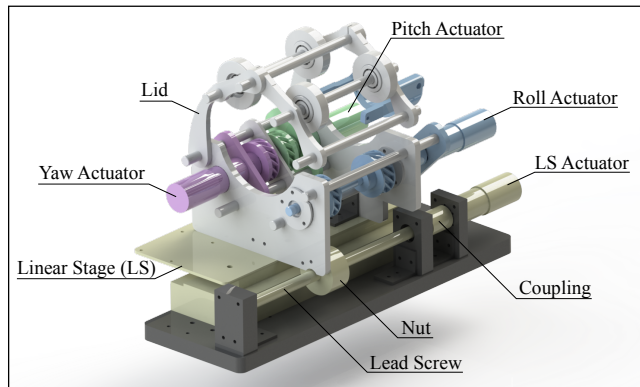


Fig. 9. CAD model showing actuator arrangement

width of the transducer adapter. The catheter handle clamp, a hinged clamp coupled to the roll driver, can then be mated to the US catheter handle and fastened with a set screw.

The alternative actuator layout method is for the pitch and yaw actuators to be mechanically grounded to the catheter handle, which decouples all four DOFs and simplifies the control since pitch and yaw can be actuated independently of other joint motions, but increases the inertial loads on the roll axis. Implementing the alternative layout requires either a longer catheter connection time or a higher part count. Therefore, we have chosen to implement the robot with rotation actuators mechanically grounded to the translation stage. The downside to the chosen actuator arrangement is that roll, pitch, and yaw motion are coupled. Roll motion causes the entire catheter to rotate, which causes the relative positions of the pitch and yaw knobs on the catheter to change, thereby bending the catheter in unwanted motion. All roll motion must therefore be accompanied by complementary pitch and yaw rotations in order to maintain the desired knob positions on the catheter handle. This necessary compensation of pitch and yaw for roll motion is calculated in the robot software. The effectiveness of pitch and yaw compensation, as well as the accuracy of motion for each joint, is examined in the experiments section.

The rotational transmission is supported in a stable configuration from the top and bottom. The bottom of the transmission is mated to the four driver gears (Figs. 8 - 9). Three of the driver gears are connected to the roll, pitch, and yaw actuators. The fourth driver gear is coupled to the roll gear and causes rotation of the front knob and the roll clamp. The top is constrained by a lid containing four rollers on ball bearings. Rollers allow free rotation of the catheter transmission without axial or radial deviation. The force between the rollers and the transmission can be adjusted by tightening or loosening the lid. Tightening the lid can improve performance by reducing gear backlash at the expense of causing increased friction and gear forces in the system.

4.4 Catheter Shaft Manipulation

In order to address two-handed manipulation of the catheter shaft, it was necessary to design a clamping mechanism which would anchor to the proximal end of the catheter. The roll clamp (Fig. 10) tightens around the catheter shaft

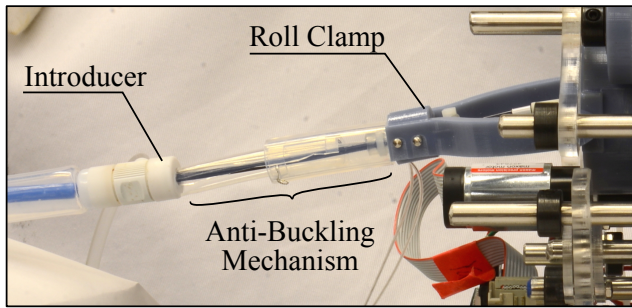


Fig. 10. Roll clamp and buckling prevention mechanisms

on the proximal end close to the catheter handle. Two connectors join the clamp to the front helical gear (A) in order to provide torsional stiffness to the catheter shaft. The front gear (A) is then coupled to the roll actuator such that all roll motion transmits torque through the front gear to the roll clamp. Transmitting torque directly to the catheter shaft (instead of relying solely on the rotation of the catheter handle) achieves a greater rotational output, thereby increasing the efficiency of roll actuation and decreasing the amount of backlash in the catheter tip due to torsional windup along the shaft.

A set of telescoping plastic tubes encases the catheter shaft between the robot and the introducer in order to prevent buckling outside the patient. The tubes were designed to have an opening along the length, allowing the telescoping assembly to be placed on or removed from the catheter shaft after the catheter has been introduced to the patient. The catheter shaft bends and presses against the inner walls of the tube assembly during insertion. The stiffness of the tubes prevents the catheter from buckling and becoming damaged. Preventing buckling outside the patient also increases the efficiency of insertion actuation. The tubes are functional even if the axes are bent at a slight angle. This gives the system robustness to variations in the alignment between the introducer and the axis of the robot during the procedure.

4.5 Robot Construction

The translation stage travels along a linear slide and is actuated by a fast-motion lead screw with pitch 1.27 cm. This joint motion can be actuated independently of the other joints. Ball bearings are attached at both ends of the lead screw to ensure smooth operation.

Each DOF is actuated by a servo-controlled brushless DC motor (EC-max, Maxon Motor, Switzerland). Motor signals (generated by the steering controller) are sent to four motor controllers (EPOS2, Maxon Motor, Switzerland), which perform fast low-level control on the motor positions of each individual actuator. The translation motor has an 84:1 gear reduction and is coupled to the lead screw by a shaft coupling. Each of the three rotational joint motors has a 53:1 gear reduction, and is connected to a smaller helical gear on the output shaft. These helical gears are mated with helical gear teeth on the Part (A-D-G-J) components of the yaw, pitch, and roll knobs. The gear ratio for each joint is 2.54. The catheter handle assembly shown in Fig. 7 is seated

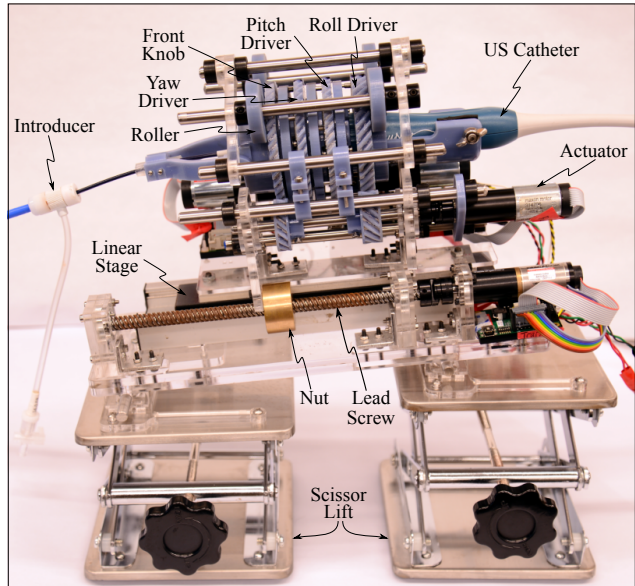


Fig. 11. Fully assembled robotic system

on top of four helical gears (Fig. 9) and held in place by the lid. Lubricant was applied to the rotational joints to reduce friction.

The knobs that engage with the catheter handle and the helical gears that connect the motors to the knobs were 3D printed (Objet Connex 500 printer, VeroBlue material, Stratasys, USA). The catheter cage, which grounds the catheter and the knobs to the translation stage, was constructed from 6.5 mm thick acrylic. The fully constructed robot is pictured in Fig. 11.

5 Experiments and Results

5.1 Transmission Accuracy

The robotic US catheter steering system depends on accurate positioning and orientation steering in order to visualize the desired anatomical features and track the clinician's working instruments. In this section we identify potential error sources resulting from mechanical design and implementation, and then we test the motion of the robot to experimentally determine its accuracy. A high-resolution optical tracking system (Claron Technology Inc., Canada) with root mean square (RMS) accuracy 0.25 mm was used to collect position measurements at roughly 20 Hz.

The linear motion of the translation axis was first examined in order to verify that the axial deviation of the nut traveling on the lead screw is as small as possible. An optical tracking marker was placed on the lead screw nut and its displacement was measured by the tracker while the translation axis was made to traverse its full 15 cm range of motion 10 times. The position measurements of the linear stage were compared with the desired straight path. The distance from each measured point to the desired straight line was calculated for each of the 4460 data points. The average deviation from the centerline was calculated to be 0.07 mm, which is less than the specified accuracy of the optical tracking sensor.

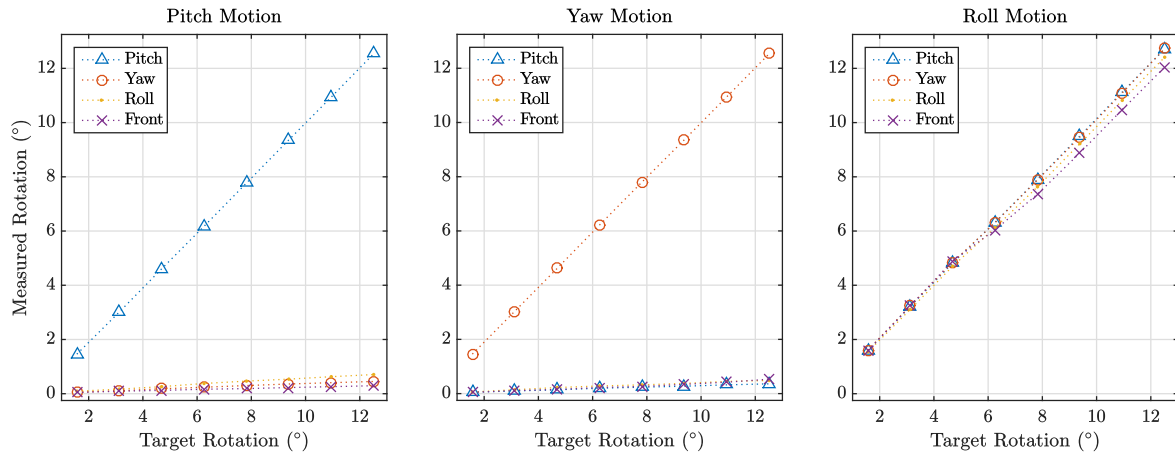


Fig. 12. Joint motion during (left) pitch, (middle) yaw, and (right) roll

Next, the backlash in the translation stage was examined. The rated backlash in the actuator gearhead is 1.6° . This amount of gearhead backlash is expected to cause up to 0.23 mm backlash (less than the specified sensor accuracy) when switching the direction of linear motion. Additionally, errors and misalignment in the mounting of the lead screw and motor shaft coupling may also contribute to the translation motion error.

The linear stage actuator was actuated to drive forwards and cause the lead screw to engage with the lead screw nut in the positive direction. Then the position of the linear stage was measured while the stage was driven forwards and backwards by a constant distance of 2.4 mm. During direction changes, a small amount of distance was lost as the lead screw rotated to engage with the threads in the opposite direction. This test was conducted 10 times with different constant distances (2.4 mm, 5.9 mm, and 11.8 mm). The average positioning error due to backlash was 0.06 mm (standard deviation = 0.03 mm), which is less than the specified accuracy of the optical tracking sensor, and is assumed to be negligible in positioning the catheter.

The rotational transmission consists of three separate actuators to rotate pitch, yaw, and roll. Friction between the ball bearings separating the three joints causes each joint to exert a small torque on neighboring joints when actuated. The resulting small joint motions are allowed by the backlash between helical gears. This effect was studied by attaching

optical tracking markers to each of the four knobs and measuring their rotations during actuation of each of the three rotational DOFs.

The results of these experiments are summarized in Table 1. First, the pitch joint was repeatedly actuated from 0° to 12.51° in increments of 1.56° . Fig. 12 (left) shows pitch knob motion and the resulting effect on the yaw, roll, and front joints. The desired pitch adjustments were achieved with mean error 0.06° (standard deviation = 0.08°). The yaw, roll, and front knobs experienced average unwanted rotation in each increment as noted in the first column of Table 1. The overall total unwanted deviation of each knob is listed as well. Second, the yaw joint was repeatedly actuated from 0° to 12.51° in increments of 1.56° . Fig. 12 (middle) shows yaw knob motion and the resulting effect on the pitch, roll, and front knobs. The desired yaw adjustments were achieved with mean error 0.04° (standard deviation = 0.05°). The resulting errors in the pitch, roll, and front knobs are in the second column of Table 1. Third, the roll joint was repeatedly actuated from 0° to 12.51° in increments of 1.56° . The pitch and yaw joints were given equal motion commands to ensure that the relative rotations of the knobs with respect to the catheter handle remained constant during roll actuation. The front knob is mechanically coupled to the roll knob through gearing and therefore should exhibit the same amount of motion as well. Fig. 12 (right) shows the resulting rotations of all four joints. The desired adjustments were achieved with mean errors listed in the third column of Table 1.

The total backlash in each rotational joint of the robot is

Table 1. Joint motion study results

		Actuated Gear		
		Pitch	Yaw	Roll
Error	Pitch	$0.06^\circ \pm 0.08^\circ$	$0.05^\circ \pm 0.03^\circ$ total: 0.36°	$0.11^\circ \pm 0.06^\circ$
	Yaw	$0.06^\circ \pm 0.03^\circ$ total: 0.45°	$0.04^\circ \pm 0.05^\circ$	$0.11^\circ \pm 0.06^\circ$
	Roll	$0.09^\circ \pm 0.04^\circ$ total: 0.71°	$0.06^\circ \pm 0.03^\circ$ total: 0.49°	$0.09^\circ \pm 0.07^\circ$
	Front	$0.04^\circ \pm 0.02^\circ$ total: 0.30°	$0.07^\circ \pm 0.04^\circ$ total: 0.53°	$0.22^\circ \pm 0.30^\circ$

Table 2. Measured backlash in each helical gear. The numbers reported below are the amount of error in joint rotations due to directional changes.

	Pitch	Yaw	Roll	Front
Mean	0.63°	0.45°	0.86°	0.18°
St. Dev.	0.01°	0.02°	0.01°	0.02°

defined as the amount of rotation lost in directional changes. This is due to a combination of the backlash in the gearhead (rated at 1.6°) and the helical gears, with fasteners and material strain contributing a negligible amount of backlash. The total backlash was measured by rotating each joint by 14.08° in different directions 10 times. Backlash results are shown in Table 2. The yaw, pitch, roll, and front knobs experienced low mean backlash.

Transmission motion testing demonstrated that the robot joints can be accurately and precisely positioned with sub-millimeter and sub-degree accuracy, which is well within the specified range. Small errors in the robot motion cause negligible errors in the catheter positioning and orientation control. The linear transmission backlash contributed negligible positioning error. The error in the rotational transmission due to backlash was 43-89% less than the allowable joint position error, 1.5° . Therefore, the joint motions are sufficiently accurate to manipulate the US catheter knobs.

5.2 Catheter Shaft Motion

The roll clamp and buckling prevention mechanisms were evaluated by repeatedly rotating and inserting the catheter in two experimental settings. The first setting (labeled “Introducer”) was on the bench top with the catheter inserted through a 14F introducer with a silicone rubber seal. The introducer was inside a smooth-walled tube (Teflon FEP,

1.3 cm inner diameter, 62 cm length). The second setting was in an *in vivo* porcine animal model during an interventional procedure with the robot. The catheter was introduced to the vasculature through a 14F introducer and the distal tip was manually guided to the junction of the inferior vena cava and the right atrium under fluoroscopic-imaging guidance. Then the catheter handle was clamped into the robot. The *in vivo* protocol was approved by the Institutional Animal Care and Use Committee (IACUC). The animal received humane care in accordance with the *1996 Guide for the Care and Use of Laboratory Animals*, recommended by the US National Institutes of Health.

For each of these two settings, tests were conducted with and without the roll clamp and the buckling mechanism. Within each setting a repeated input was given to the robot and the resulting motion of the catheter tip was measured as output. The ratio of catheter tip output motion to catheter handle input motion is less than one in all cases, even with mechanical assistance from the roll clamp and the buckling prevention tubes. During roll tests, this is due to friction on the catheter shaft causing torsional windup along the length of the shaft. During insertion tests this is due to two factors: (A) friction on the catheter shaft from the rubber seal of the introducer, which increases the amount of shaft buckling before the shaft stiffness overcomes the friction in the rubber seal, and (B) deformation of the catheter shaft as it conforms to the contour of the tubing before it begins to slide in through the rubber seal. Fig. 13 shows the performance of the roll clamp, and Fig. 14 shows the performance of the buckling mechanism in each setting. The results of the handle insertion and rotation tests demonstrated that the roll clamp and buckling prevention tubes improved the effectiveness of the robot motion. During *in vivo* trials robot alignment with the introducer was subject to small shifts over time. Without the buckling prevention tubes, this misalignment combined with introducer friction caused the catheter shaft to buckle, thereby transmitting near zero translation to the distal tip of the catheter. The use of buckling prevention tubes was necessary in order to steer the catheter *in vivo*.

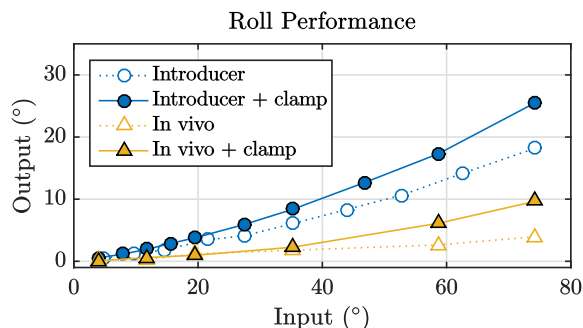


Fig. 13. Relationship between handle roll input and catheter tip roll output

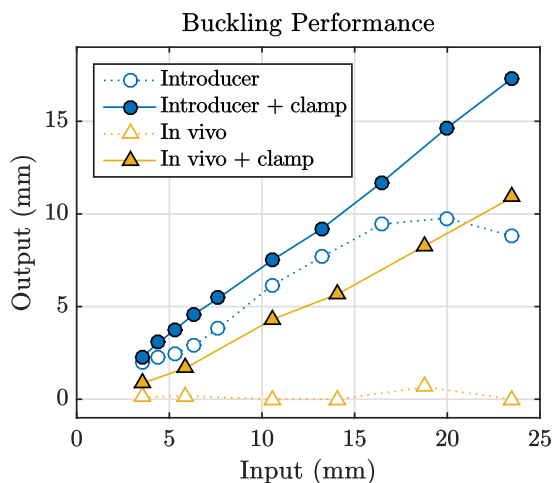


Fig. 14. Relationship between handle insertion input and catheter tip translation output

6 Navigation and Control

The above hardware can be used to control the imaging catheter tip positioning and imager angle by a variety of methods [3–5]. In general, direct sensing of the tip location is needed to deal with the challenging behavior of the polymer catheter shaft as well as the *in vivo* vasculature environment. Here we describe our most recent sensing and control strategy. The robot is navigated by an iterative process pictured in the diagram of Fig. 15. Inverse kinematics calculations map the current measured pose (using EM sensors) to a set of estimated current joint space angles. The desired pose is also mapped to a set of desired joint space angles. The relative difference between the two sets of joint space angles is input to the joint controllers and the robot steers the catheter. The tip pose is then measured again to find the new estimated current joint space angles and this process iterates until the catheter tip converges to the desired pose. Information from

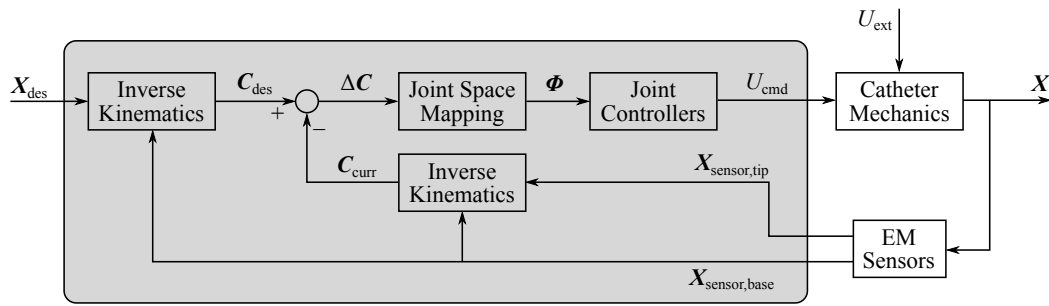


Fig. 15. The controller (gray box) receives the desired catheter tip pose and iteratively calculates joint angle adjustments to manipulate the catheter

the distal tip EM sensor is necessary in order to measure the pose of the tip. Information from the distal base EM sensor is necessary in order to measure the amount of true roll experienced at the bending section of the catheter. It is not possible for the kinematics calculations to use the motor joint angles reported by the encoders, because the effects of friction and nonlinearities in the catheter body significantly reduce the accuracy of joint-to-tip space mappings.

Benchtop experiments demonstrated automatic catheter tip steering along a square trajectory of 4 cm on each side. The full desired pose was specified for each target point along the trajectory. Position results are shown in Fig. 16. The mean position error was 0.92 mm (standard deviation = 0.12 mm) and the mean angular error was 1.01° (standard deviation = 1.01°).

Tip control was also demonstrated during *in vivo* trials on a porcine animal model, by accurately maintaining a fixed position while adjusting the US imager. During the study, respiratory and cardiac motion caused the catheter tip and body to displace cyclically. Physiological effects during breath hold cause the heart to displace at a slow continuous rate. This means that the catheter body is still subject to lung-related disturbance during breath hold. It is not possible to navigate square trajectories due to patient cardiac safety, therefore in this set of tip navigation tests, the catheter was commanded to maintain a fixed pose in space (with respect to the world frame) while the patient's breath was held. Fig. 17 shows an example test in which the position and imager angle maintained the fixed pose in the world frame despite cardiac and lung motion. The position was commanded to remain fixed while the imager was given a step input at $t = 7$ s of 2°. This causes a jump in the reported angular

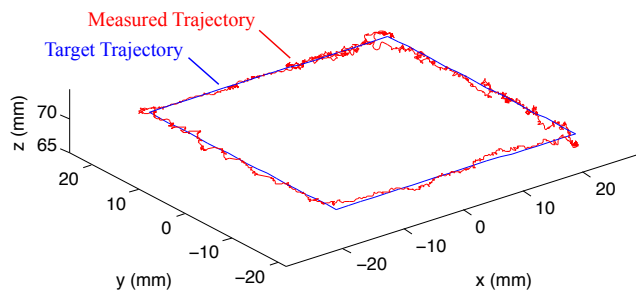


Fig. 16. Bench top catheter tip navigation of a square trajectory

error, which is then mitigated by the controller performing the angle adjustment. The mean position error was 1.3 mm (standard deviation = 0.6 mm) and the mean angular error was 0.71° (standard deviation = 0.49°).

7 Conclusions and Future Work

An accurate actuation module is necessary for providing a clinically relevant robotic system for steering US catheters. In our study, we have demonstrated that our new robotic system satisfies the desired accuracy specifications. The level of accuracy required was determined by the relationships between joint inputs and catheter tip outputs. Measurements of the robot motion with the high-resolution optical tracker demonstrated that the robot is capable of positioning its joints and the catheter tip pose with sub-millimeter and sub-degree level accuracy. These errors are the results of friction in custom designed ball bearing joints, small inaccuracies in the fabrication and assembly stages of the robot, limited resolution of encoders that measure the motor positions, limited resolution of the optical tracker, and noise in the experimental setting. Based on the results of robot motion experiments, we have demonstrated that the errors in the physical implementation of the robot are small enough for

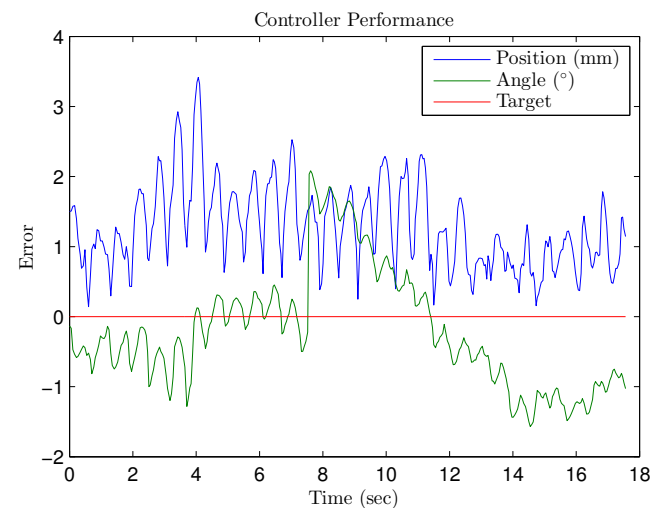


Fig. 17. *In vivo* catheter tip navigation to maintain fixed position during imager angle adjustment. A 2° step input was given to the controller at $t = 7$ s.

the robotic system to be useful. Many of the joint motion errors were measured to be less than the specified accuracy of the optical tracker. A more accurate sensor would be necessary in order to more accurately measure the joint-level positioning ability of the robot.

The robotic system presented here offers a smaller footprint than our previous system, which is crucial for a clinically-feasible robot. The attachment and detachment procedure for the US catheter enables quick connect and disconnect from the robotic system. The roll clamp and buckling prevention mechanisms improve the output/input ratio (efficiency) of catheter tip motions to handle inputs. Experimental validation of the actuation module has demonstrated that the US catheter can be manipulated with sufficient accuracy to achieve enhanced visualizations during catheter-based procedures.

Acknowledgements

This work was supported by the Harvard School of Engineering and Applied Sciences, American Heart Association Grant #15PRE22710043, and NIH grant #1R21EB018938.

References

- [1] Moscucci, M., 2013. *Grossman & Bain's Cardiac Catheterization, Angiography, and Intervention*. Lippincott Williams & Wilkins.
- [2] Intracardiac Echocardiography. [Online]. Available: <http://www.eplabdigest.com/article/4148>.
- [3] Loschak, P., Brattain, L., and Howe, R., 2013. "Automated pointing of cardiac imaging catheters". In *Robotics and Automation (ICRA), 2013 IEEE Int'l Conf. on*, pp. 5794–5799.
- [4] Loschak, P. M., Brattain, L. J., and Howe, R. D., 2014. "Algorithms for automated pointing of cardiac imaging catheters". In *Computer-Assisted and Robotic Endoscopy*. Springer, pp. 99–109.
- [5] Brattain, L. J., Loschak, P. M., Tschabrunn, C. M., Anter, E., and Howe, R. D., 2014. "Instrument tracking and visualization for ultrasound catheter guided procedures". In *Augmented Environments for Computer-Assisted Interventions*. Springer, pp. 41–50.
- [6] Loschak, P. M., Tenzer, Y., Degirmenci, A., and Howe, R. D., 2015. "A 4-dof robot for positioning ultrasound imaging catheters". In *Proc. ASME International Design Engineering Technical Conf and Computers and Information in Eng Conf, IDETC CIE* (in press).
- [7] Catheter Robotics, Inc. *Amigo Remote Catheter System*. [Online]. Available: <http://catheterrobotics.com/images/AmigoBrochure.pdf>.
- [8] Corindus, Inc. *CorPath Robotic PCI*. [Online]. Available: <http://www.corindus.com/>.
- [9] Hansen Medical, Inc. *Sensei X Robotic Catheter System*. [Online]. Available: <http://hansenmedical.com>.
- [10] Stereotaxis *Niobe ES*. [Online]. Available: <http://www.stereotaxis.com/products/niobe/>.
- [11] Stereotaxis *V-Drive Robotic Navigation System*. [Online]. Available: <http://www.stereotaxis.com/products/vdrive/>.
- [12] Creighton, F., Ritter, R., Viswanathan, R., Kastelein, N., Garibaldi, J., and Flickinger, W., 2009. "Operation of a remote medical navigation system using ultrasound image". US2009/0062646 A1.
- [13] Webster III, R. J., and Jones, B. A., 2010. "Design and Kinematic Modeling of Constant Curvature Continuum Robots: A Review". *Int'l J of Robotics Research (IJRR)*, **29**(13), pp. 1661–1683.
- [14] Khoshnam, M., Azizian, M., and Patel, R. V., 2012. "Modeling of a steerable catheter based on beam theory". In *Robotics and Automation (ICRA), 2012 IEEE Int'l Conf. on, IEEE*, pp. 4681–4686.
- [15] Ganji, Y., Janabi-Sharifi, F., and Cheema, A. N., 2009. "Robot-assisted catheter manipulation for intracardiac navigation". *Int'l J of Comp. Asst. Radiology and Surgery*, **4**(4), pp. 307–315.
- [16] Camarillo, D. B., Carlson, C. R., and Salisbury, J. K., 2009. "Configuration tracking for continuum manipulators with coupled tendon drive". *Robotics, IEEE Trans. on*, **25**(4), pp. 798–808.